ALT-3 LINER-TARGET INTERACTION

A. G. Sgro and C. L. Rousculp

Los Alamos National Laboratory, Los Alamos, NM 87545, USA

The ALT-3 experiment will measure the equation of state (EOS) of a cylindrical target which is hit by a cylindrical imploding liner. Previous simulations of the liner implosion without the target included have found that the part of the liner immediately adjacent to the axial glide planes (which bound the axial extent of the volume internal to the liner) creates a jet which runs ahead of the rest of the liner and reaches the position of the target first. This presentation will include the target and will describe and summarize two dimensional simulations of the liner- target interaction, which is driven by the expected axial current profile. One of the simulations presented herein will show that the part of the target hit by the jet in turn hits the central measuring unit (CMU) before the rest of the target does. This will damage the CMU and may endanger data collection. Other simulations will show how various features (a small "tooth" in the glide plane close to the target as designed by A. Buyko, or small rings of various materials covering the target next to the glide plane), can prevent damaging the CMU before data collection is complete. A previous report has summarized results of one dimensional simulations of the interaction and reported on the velocity of the inner liner surface at the radius of the target, the velocity of the shock in the target, and the jump off velocity of the inner target surface after the shock reaches it, and the resulting determination of the EOS parameter for the "computational Aluminum" in the simulation. The 2 dimensional simulations produce very similar results for these velocities and the EOS parameter.

Introduction

Dynamic material science experiments, especially those at extreme pressure, temperature, and density, may require large amounts of energy to be converted to particle kinetic energy and delivered with high precision. Electromagnetic energy sources offer significant advantages in precision, controllability, reproducibility, and sometimes even energy, over other drivers for some experiments. Both magnetically imploded, cylindrical liners and magnetically driven planar impactors have met the requirements for precision on high performance laboratory sources. Two explosive pulse compression systems, capable of even larger energies have emerged as attractive drivers, especially for liner driven shock physics, materials EOS, and constitutive properties. These systems are the Disk Explosive Magnetic Generator (DEMG) developed at VNIIEF, and the Coaxial Flux Compression Generator (Ranchero) developed at LANL.

Cylindrical Liners

The cylindrical, imploding liner is perhaps the most thoroughly studied mechanism for converting electrical energy into the particle kinetic energy needed for shock physics and high energy density applications.

Techniques producing 20-30 MJ of liner kinetic energy (at 5-8 MJ/cm) with velocities approaching 10 km/sec have been demonstrated. Systems can be designed to achieve even higher liner velocities. Liner implosion techniques, compressing an initially solid target, can convert many megajoules of liner kinetic energy into internal energy, producing warm dense matter with only modest requirements on liner precision. In hydrodynamic design calculations, an aluminum liner at 10 km/sec (2 MJ/cm) compresses a (matched) Al target to 8 gm/cc (~3 times normal density) and energy densities approaching 140 kJ/gm (>1MJ/cc), at a few eV, and maintains the conditions for several hundred nanoseconds. Compressing the Al sample between a tungsten liner (10 km/sec) and a tungsten core could achieve Al densities of 10 gm/cc (> 4 times normal) and 150 kJ/gm (1.5MJ/cc).

However, shock physics and materials experiments, while sometimes relaxing the need for total energy, place much more stringent requirements on precision.

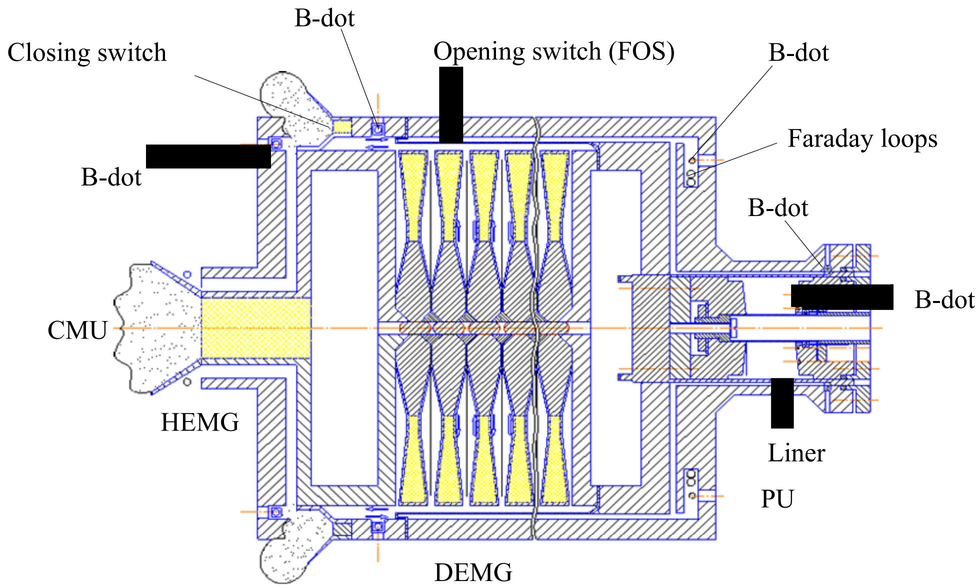

Figure 1. The DEMG with the load attached on the right

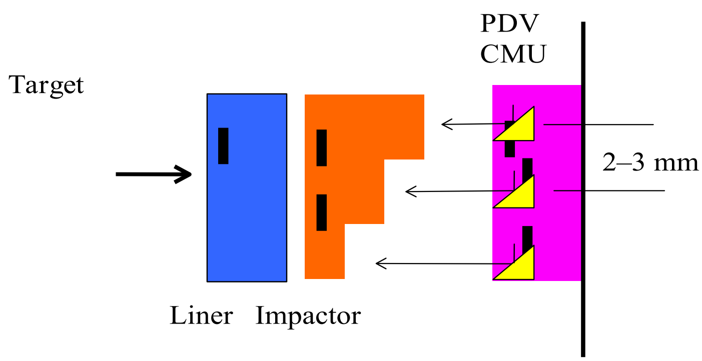

- **Approximately 32 probes**
- **8 probes for liner at 2 axial stations**
- **24 probes => 8 targets using 3/tgt**
- **2 materials, 4 measurements**

Figure 2. Sketch of the experiment

For very large energies, LANL teamed with VNIIEF in 1996 to conduct the High Energy Liner (HEL-1) experiment producing a world record liner implosion kinetic energy with a 100-MA current drive. With more than 50 % of the 1-kg liner mass unmelted, 2D effects were manifested (computationally) primarily in “end plane run-ahead.” Experimental measurements were consistent. The liner velocity at the central measuring unit (CMU) was 6.7 km/sec – 8.4 km/sec. The liner kinetic energy at the CMU (4:1 radial convergence) was between 22 MJ and 35 MJ.

Terapascal Equation of State (EOS) Experiment

LANL and VNIIEF are collaborating in the design of a cylindrical terapascal EOS experiment based on a 60 MA, 20 km/sec, imploding liner powered by a Disk Explosive Magnetic Generator (DEMG), see Figure 1. The experiment itself, called the Advanced Liner Technology Experiment, **ALT-3**, similar to the ALT-1&2 experiments[1], is inside the load on the right side and consists of a liner (initially 0.3 cm thick with a 4 cm outer radius (OR)), a target (an 0.8 mm shell of OR 1 cm, with some thinner notched regions), a CMU, and associated hardware. The liner and the space inside it are axially bounded by two copper end walls often called glide planes (GP). A sketch of ALT-3 is shown in Figure 2.

The Influence of Glide Plane Shape on Implosion Quality

Significant effort has been devoted to the development of the optimal glide plane shape for ALT-3[2–9] in order to minimize the perturbation level on the inner surface of the liner just before it impacts the target. Our previous simulations included the liner and glide plane and examined the perturbation levels when the inner liner surface reached a radius of 1 cm, the initial position of the outer surface of the target. These simulations have found that a perturbation of about 100 μm is expected on most of this surface. However, the part immediately adjacent to the glide planes creates a jet which runs ahead of the rest of the liner and impacts the target first.

Interaction of the Liner and Target

This report describes 2-D Eulerian AMR simulations which enhance our previously reported ones by including the target in the calculation. The effect of the jet on the target and the CMU, and ways to mitigate these effects, are examined. The minimum cell resolution is 50 μm and the liner is driven by a prescribed axial current (J4).

Interaction of the Liner and Target – Effect of the Jet

To illustrate the effect of the jet, the first simulation calculates the target-liner interaction with

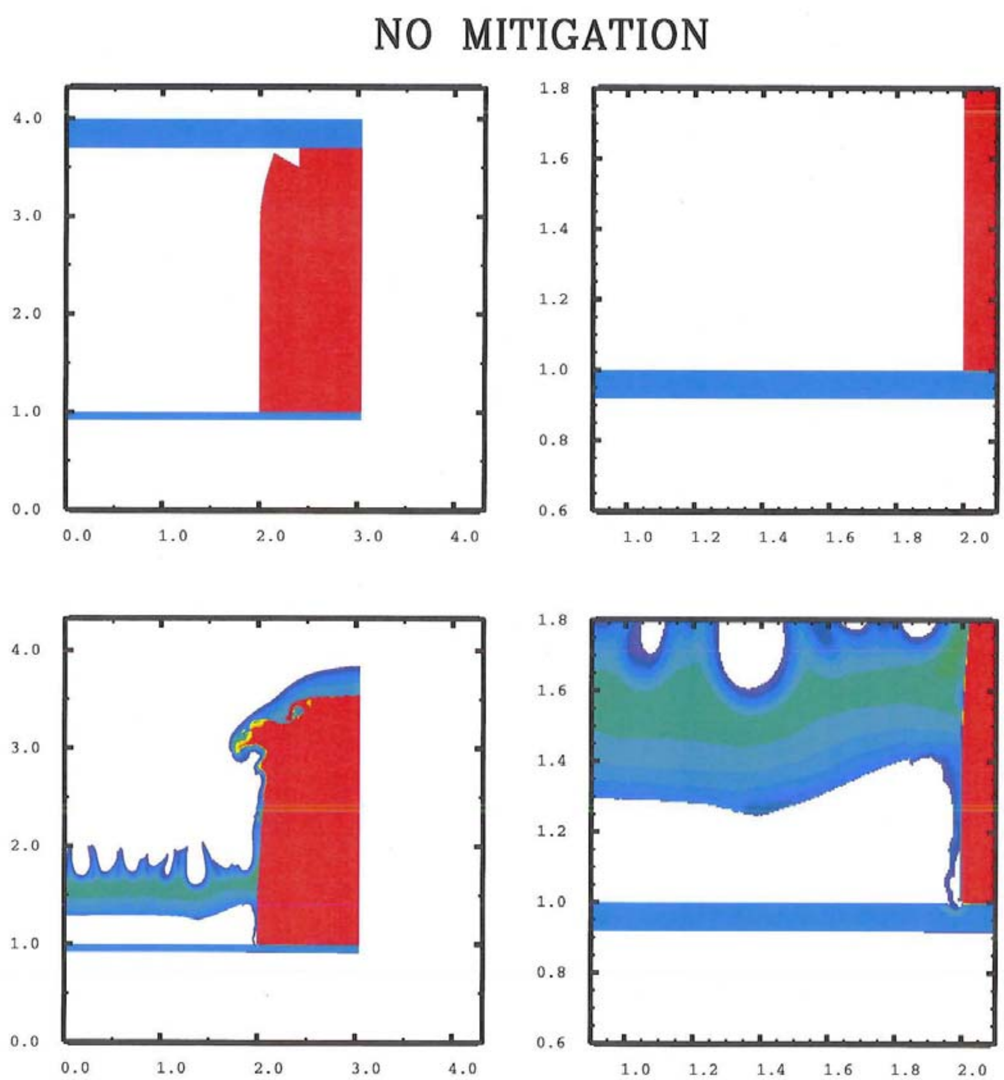

Figure 3. Target-Liner interaction with no jet mitigation. The top row shows the initial conditions and the bottom row shows the time when the jet first reaches the target

no attempt to mitigate the jet. The following figures show density plots and have two columns. The left hand column presents the full region of the simulation and the right hand column presents an expanded view of the interaction region, from 0.6 cm < r < 1.8 cm and 0.9 cm < z < 2.1 cm. In figure 3, the top row presents density plots of the initial conditions. . The Aluminum liner is between 3.7 cm < r < 4 cm and is colored blue. The copper end wall is red and the glide plane is the left surface of the end wall. Since the target is also Aluminum, and thus the same initial density as the liner, it is also blue and is located at 0.92 cm < r < 1.0 cm. In this figure, the outer surface of the CMU would be at 0.8 cm. Since the CMU is a highly non axisymmetric measuring device, it was not included in these axisymmetric calculations. The bottom row shows the time when the top of the jet first reaches the top of the target. Note that the liner is still ~3 mm away from the target.

The top row of figure 4 shows the time when the shock in the target due to the jet reaches the bottom of the target. Note that the liner is still ~2 mm from the target. The bottom row shows the time when the jet pushed the target ~0.5 mm inward, so that this feature is just ~0.7 mm away from the CMU. Note that the liner is still ~0.7 mm from the target.

The top row of figure 5 shows the time when the target material pushed by jet reaches outer radial position of CMU (8 mm). Beyond this time the measurements are potentially compromised. Note that the shock due to the liner is still traveling through target and has not yet broken out. The bottom row

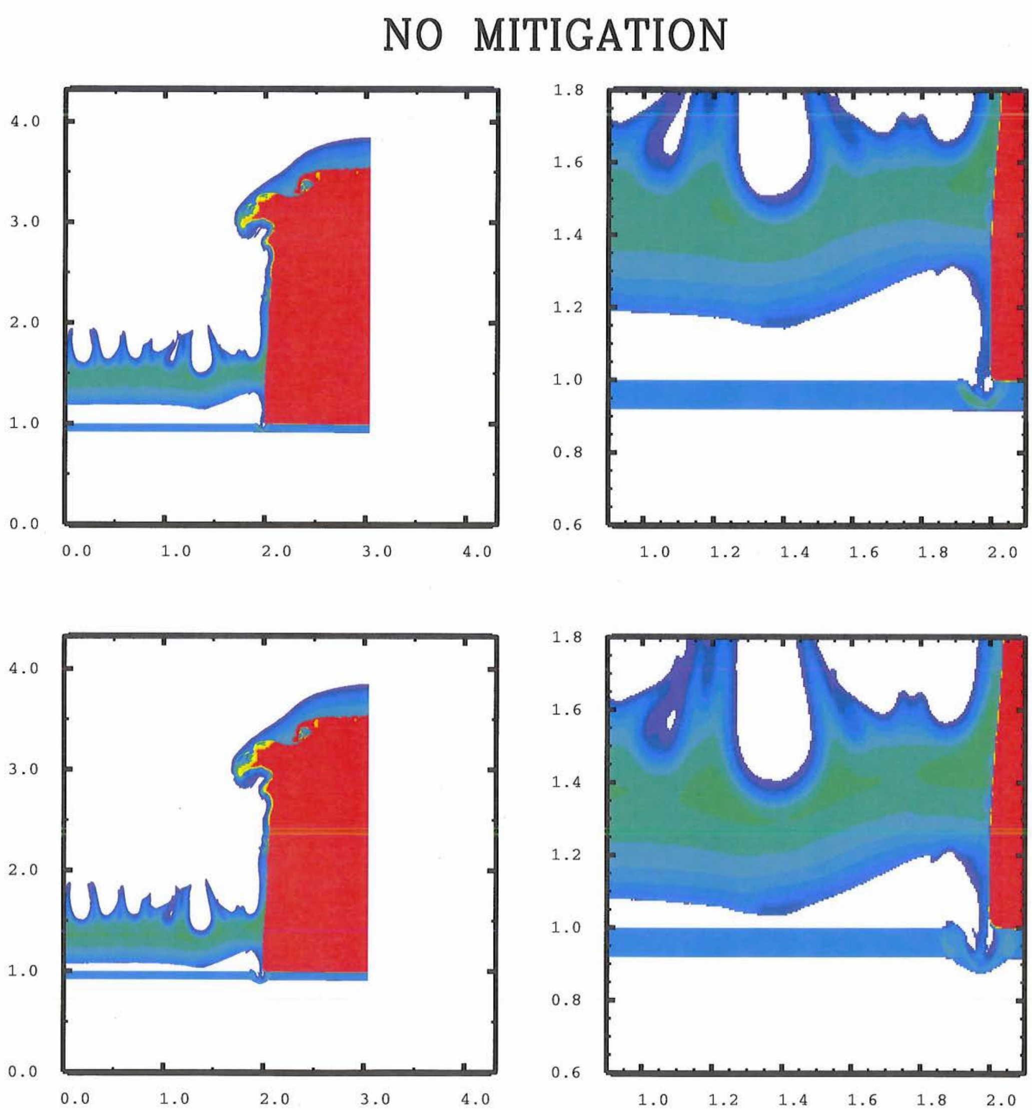

Figure 4. Target-Liner interaction with no jet mitigation. Top row: the shock from the jet reaches the bottom of the target. Bottom row: the jet pushes the bottom of the target ~0.5 mm inward.

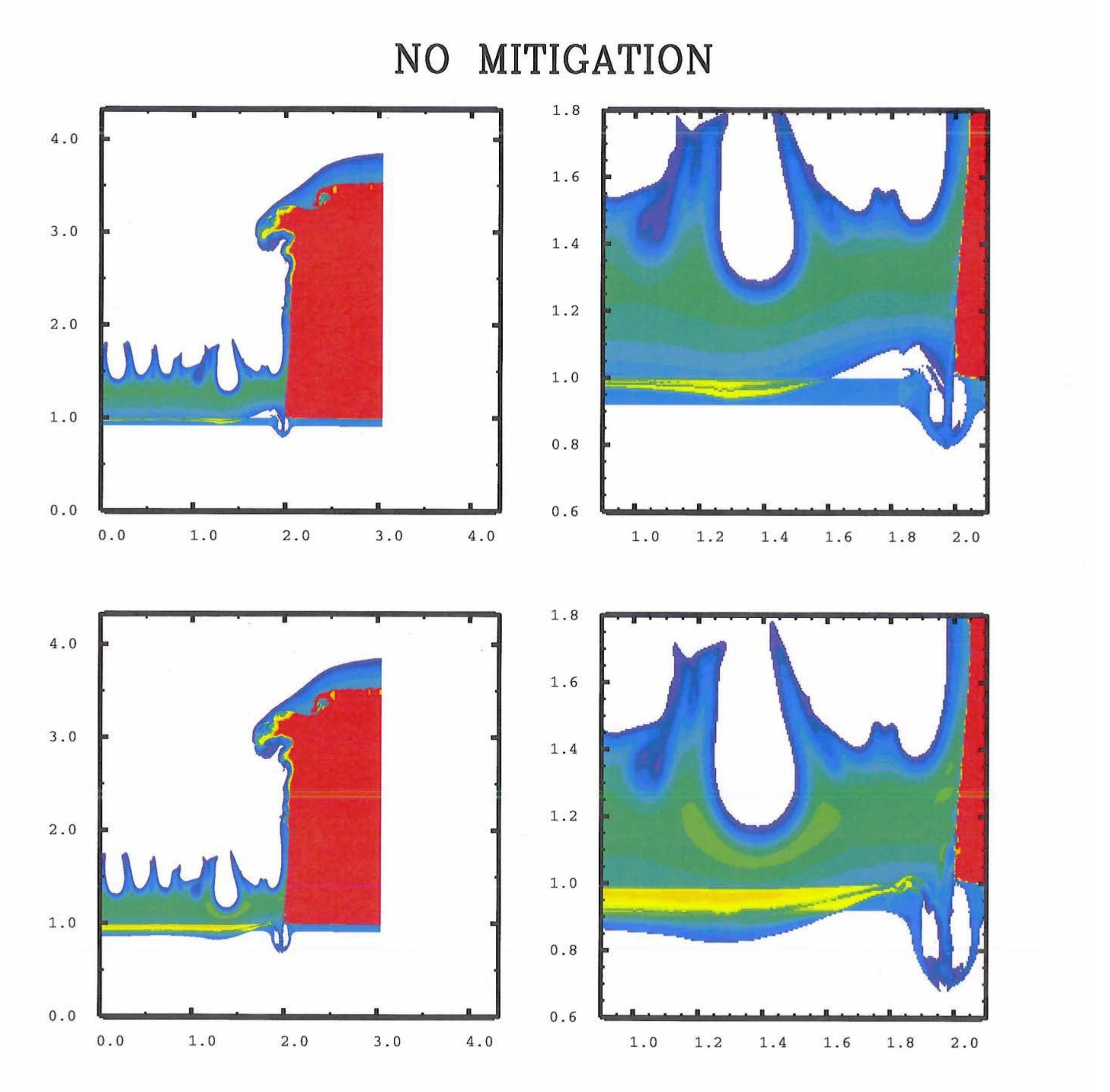

Figure 5. Target-Liner interaction with no jet mitigation. Top: Target material pushed by jet reaches outer radial position of CMU. The shock due to liner is still traveling through target. Bottom: Target pushed by the jet is deep into CMU location. The inner target surface has not yet reached the position of the CMU.

of this figure shows the time when the target has pushed by jet deep into CMU location. Note that the inner target surface has not yet reached the position of the outer surface of the CMU. This simulation shows that the data collection is potentially compromised without mitigation of jet.

The next few sections will examine various possibilities to mitigate the potential effect of the jet on the CMU. The basic idea of all the mitigation attempts is to put extra mass between the liner and the target at the expected axial position of the jet, in order to slow it down.

Target-Liner Interaction with Tooth Notch

One idea for mitigating the influence of the jet is to include a notch in the glide plane, as designed by Buyko[10]. This is illustrated in the top row of figure 6, which shows the initial conditions of the simulation. The notch is at r ~1.2 cm, 1.8 cm < z < 2.0 cm. The bottom row of this figure shows the time when the jet first reached the top of the notch. At this time the tip of the jet is far ahead of the rest of the liner.

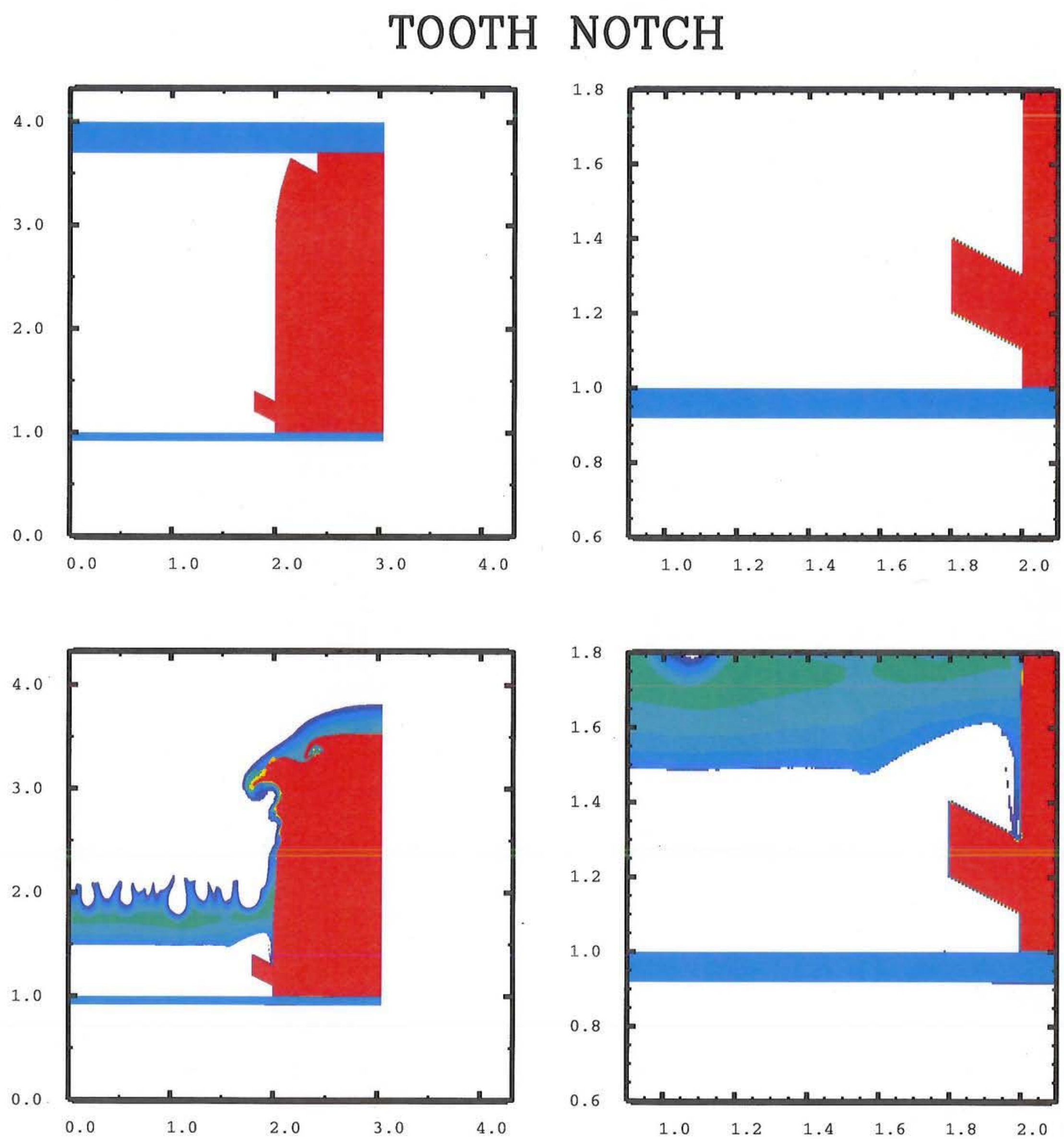

Figure 6. Target-liner interaction with a tooth notch[10]. Top row: initial conditions. Bottom row: tip of jet reaches top of notch. The tip of the jet is ahead of the rest of the liner

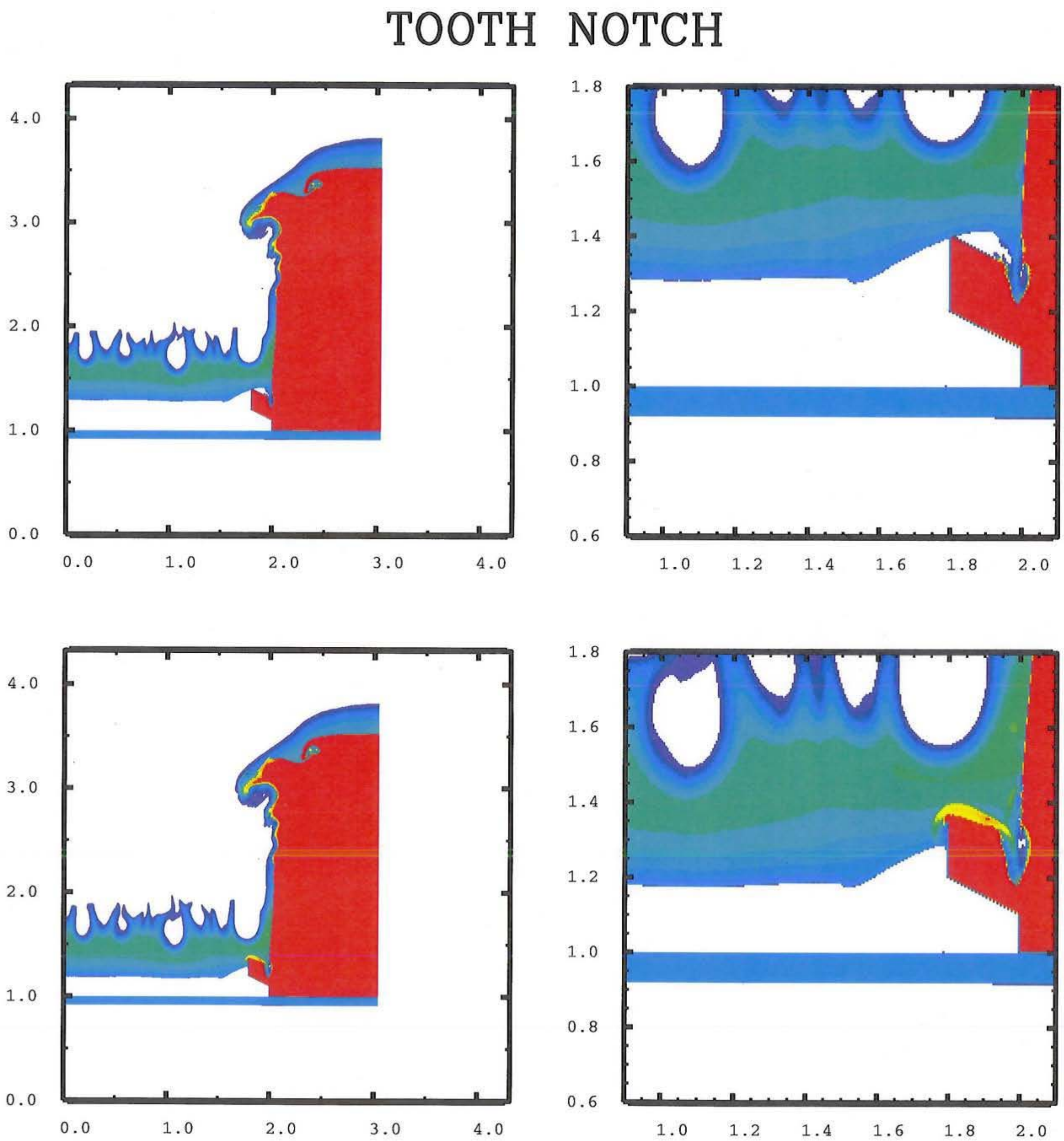

Figure 7. Target-liner interaction with a tooth notch[10]. Top: The jet slows down as it plows through notch. The rest of liner starts to catch up. Bottom: The jet still is still restrained by notch. The rest of liner starts to pass the jet

Figure 7 shows the continuation of the interaction. The top row shows that the Jet slows down as it plows through the extra mass of the notch while the rest of liner starts to catch up. The bottom row shows that the jet is still restrained by notch while the rest of liner starts to pass the jet.

Figure 8 presents the conclusion of this run. The top row shows that the jet still constrained by notch even as the rest of the liner has already hit the target and the resulting shock is traveling through target. The bottom row shows that as the liner approaches the top of CMU position, and the experiment almost over, the jet is still constrained by notch. Thus, in the design by Buyko [10] the jet does not interfere with measurement.

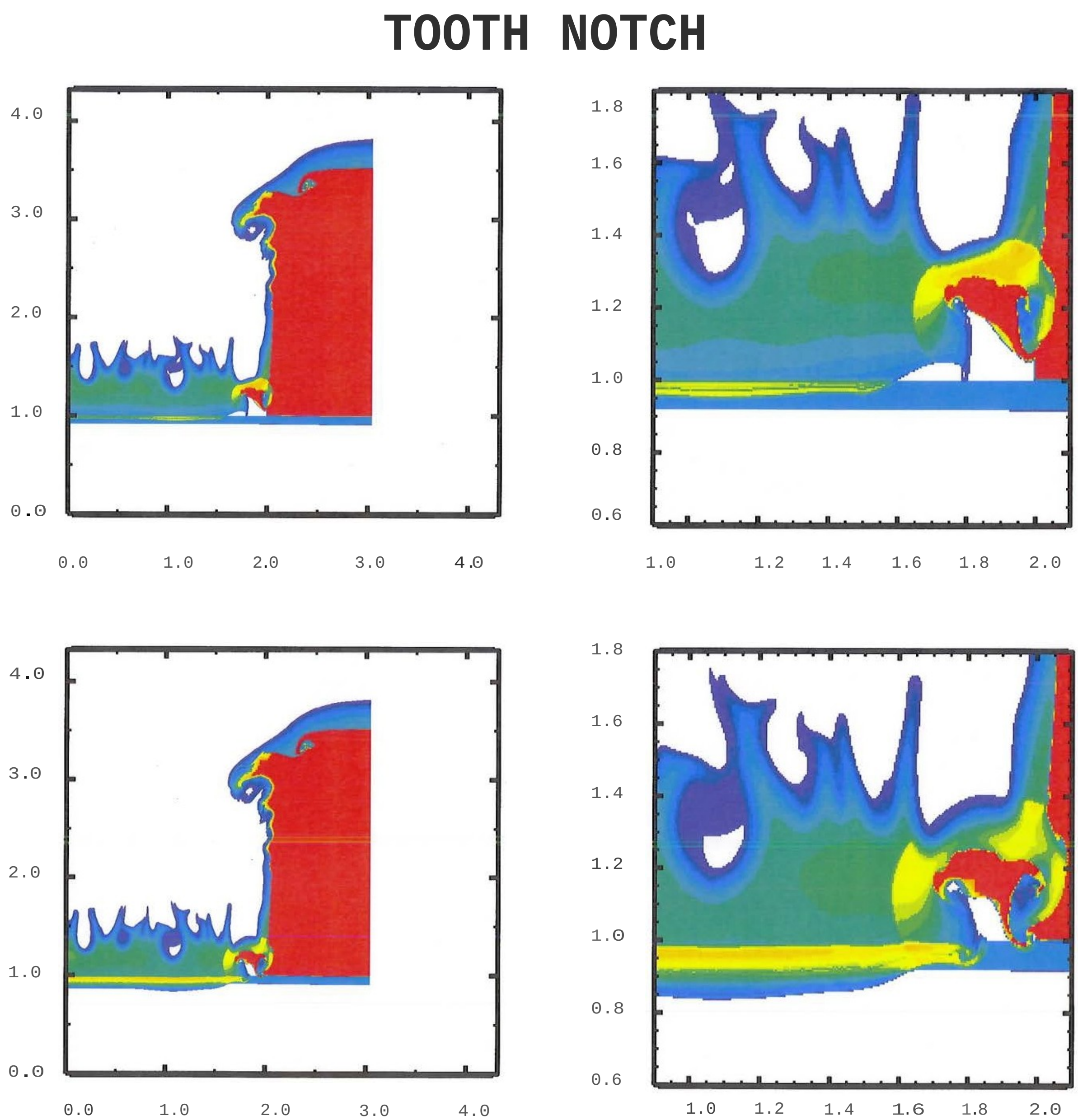

Figure 8. Interaction concludes- jet does not interfere with measurement. Top: Liner hits target and shock is half way through target. Jet still constrained by shell. Bottom: Liner almost reaches top of CMU position. Experiment almost over. Jet still constrained by notch and does not interfere with measurement.

Target-Liner Interaction with TA shell surrounding Target

Another way to put mass between the jetted region of the liner and the target is to put a ring of material around the target at the expected position of the jet. The top row of figure 9 shows the initial configuration with a ring of TA surrounding the target. In this figure, because the density of TA is much higher than that of CU, the graphics colors the CU green and the TA red. The bottom row of this figure shows the time when the jet first reaches the outer surface of the ring. Again in this calculation, the jet is far ahead of the rest of the liner

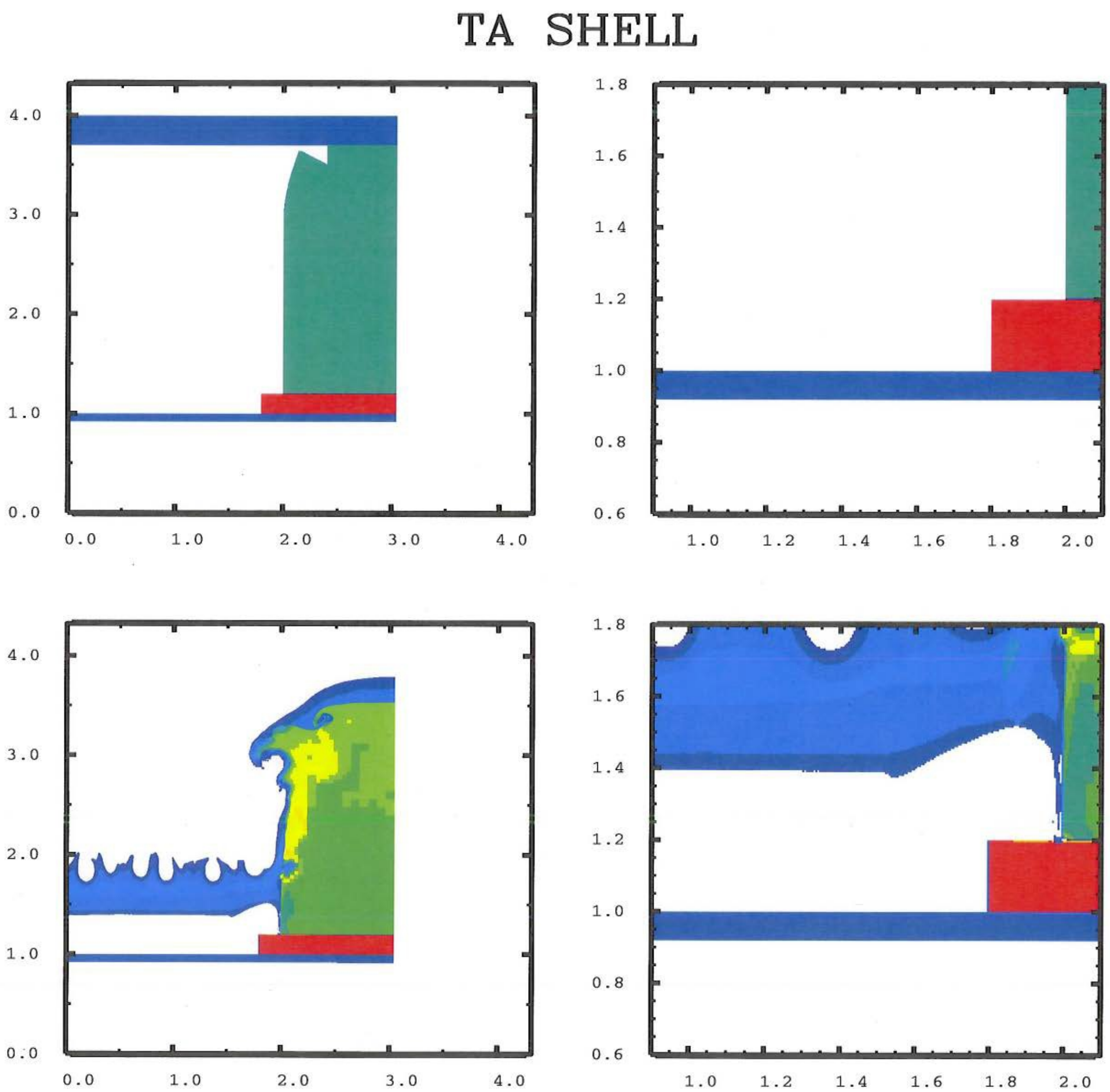

Figure 9. Target-Liner Interaction with TA ring surrounding Target. Top row: initial conditions. Ta ring surrounds target near GP. The graphics colors the Ta ring red and the GP green. Bottom row: tip of jet reaches shell. The jet is far in front of rest of liner.

Figure 10 shows this interaction continuing. The top row shows the jet slowing down as it plows through the ring, while the rest of liner starts to catch up. The bottom row shows the jet still restrained by the ring while the rest of liner starts to pass the jet.

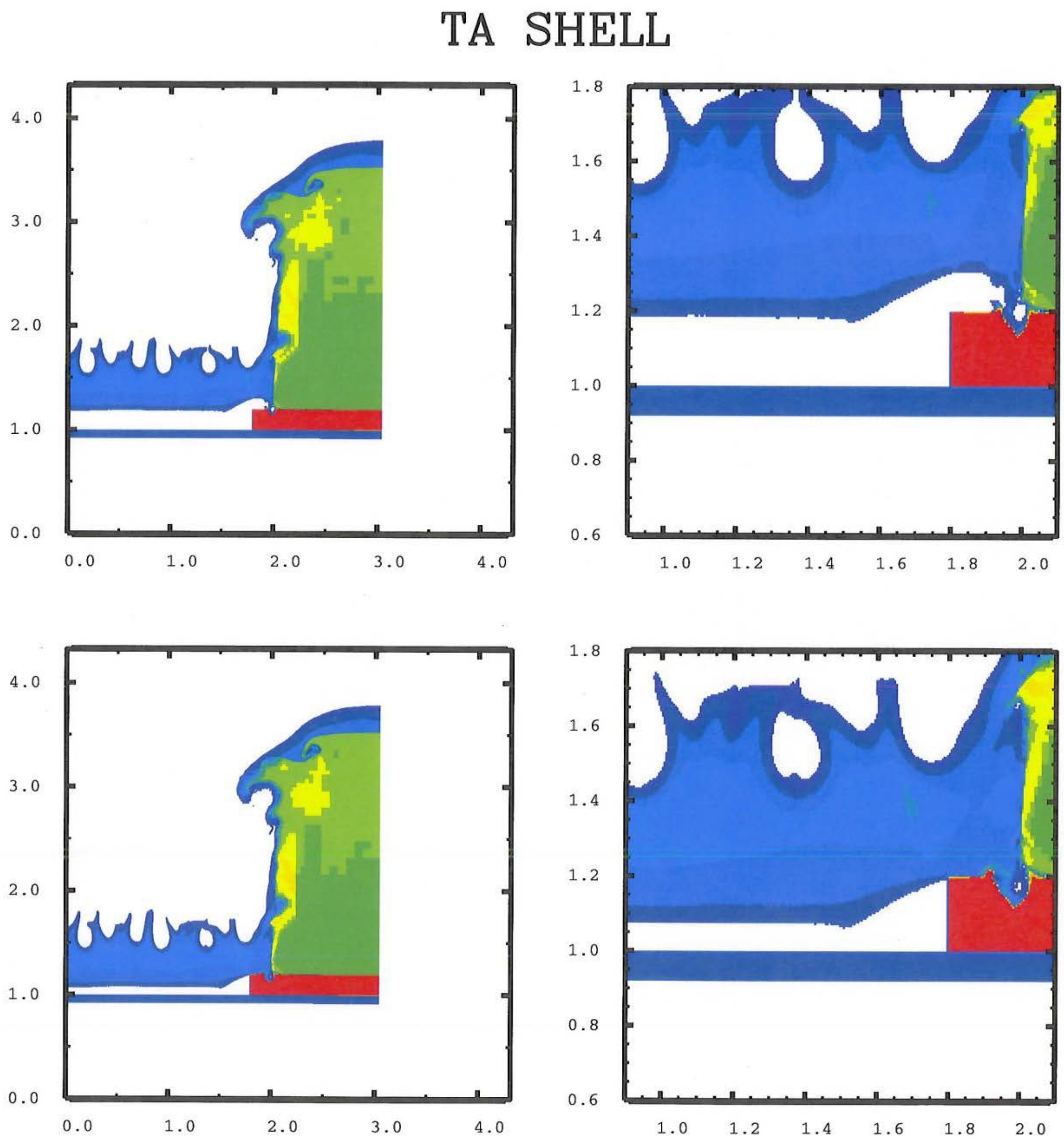

Figure 10. The interaction continues. Top: Jet slows down as it plows through the ring. Rest of liner starts to catch up. Bottom: Jet still restrained by the ring. Rest of liner starts to pass the jet.

Figure 11 shows the interaction concluding. The top row shows that after the liner hits the target and the shock travels half way through, the jet is still constrained by the ring. The bottom row shows the liner just about reaching the top of CMU position so the experiment is almost over. The jet is still constrained by the ring and does not interfere with measurement.

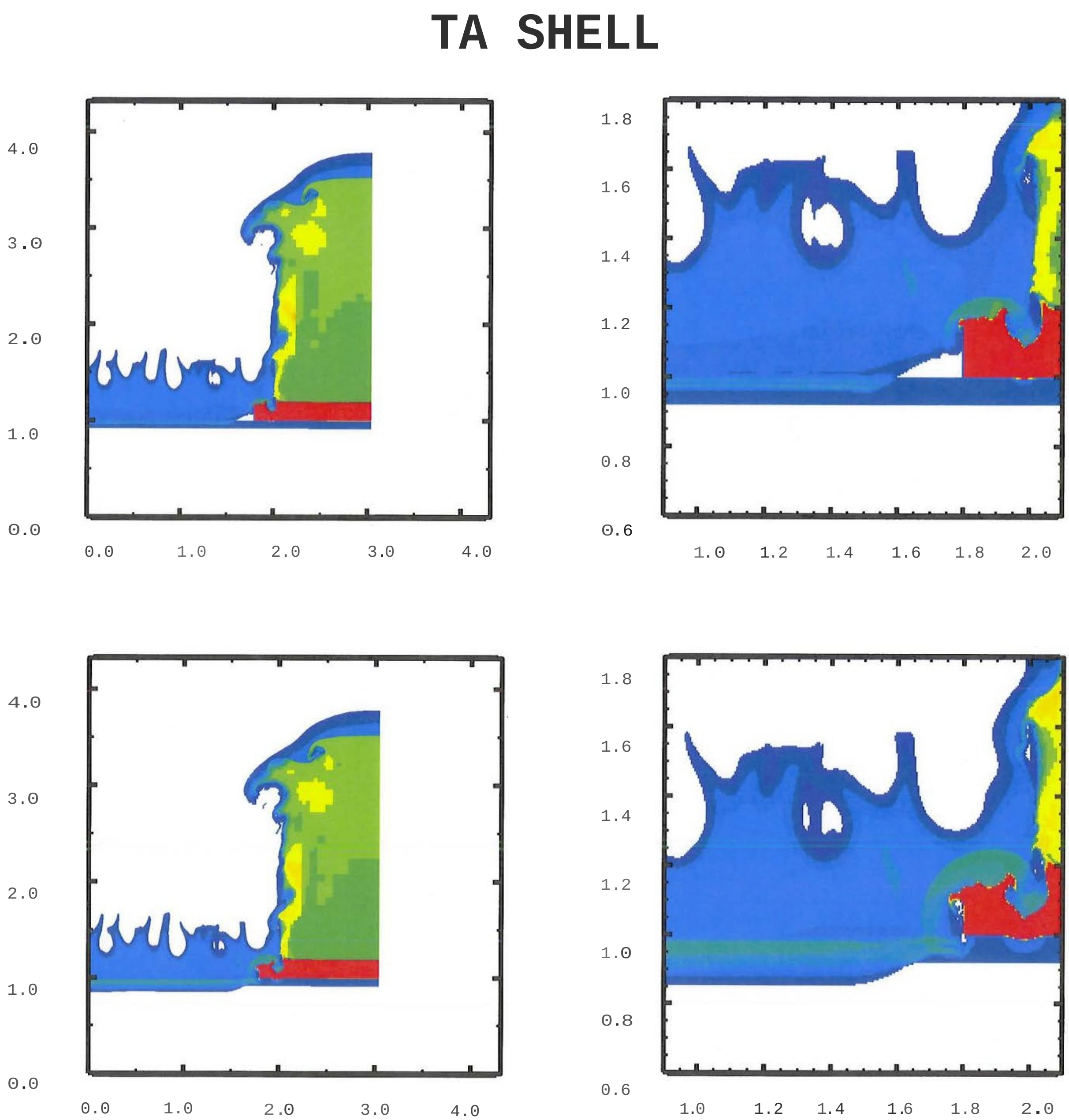

Figure 11. Interaction Concludes – Jet does not interfere with Measurement. Top: After liner hits target and shock is halfway through target. Jet still constrained by ring. Bottom: Liner almost reaches top of CMU position. Experiment almost over. Jet still constrained by the ring and does not interfere with measurement.

Target-Liner Interaction with CU shell surrounding Target

Another possibility is to surround the target with a CU ring. The top row of figure 12 shows the initial conditions of such a configuration and the bottom row shows the time when tip of jet reaches the ring. The jet is far in front of rest of liner.

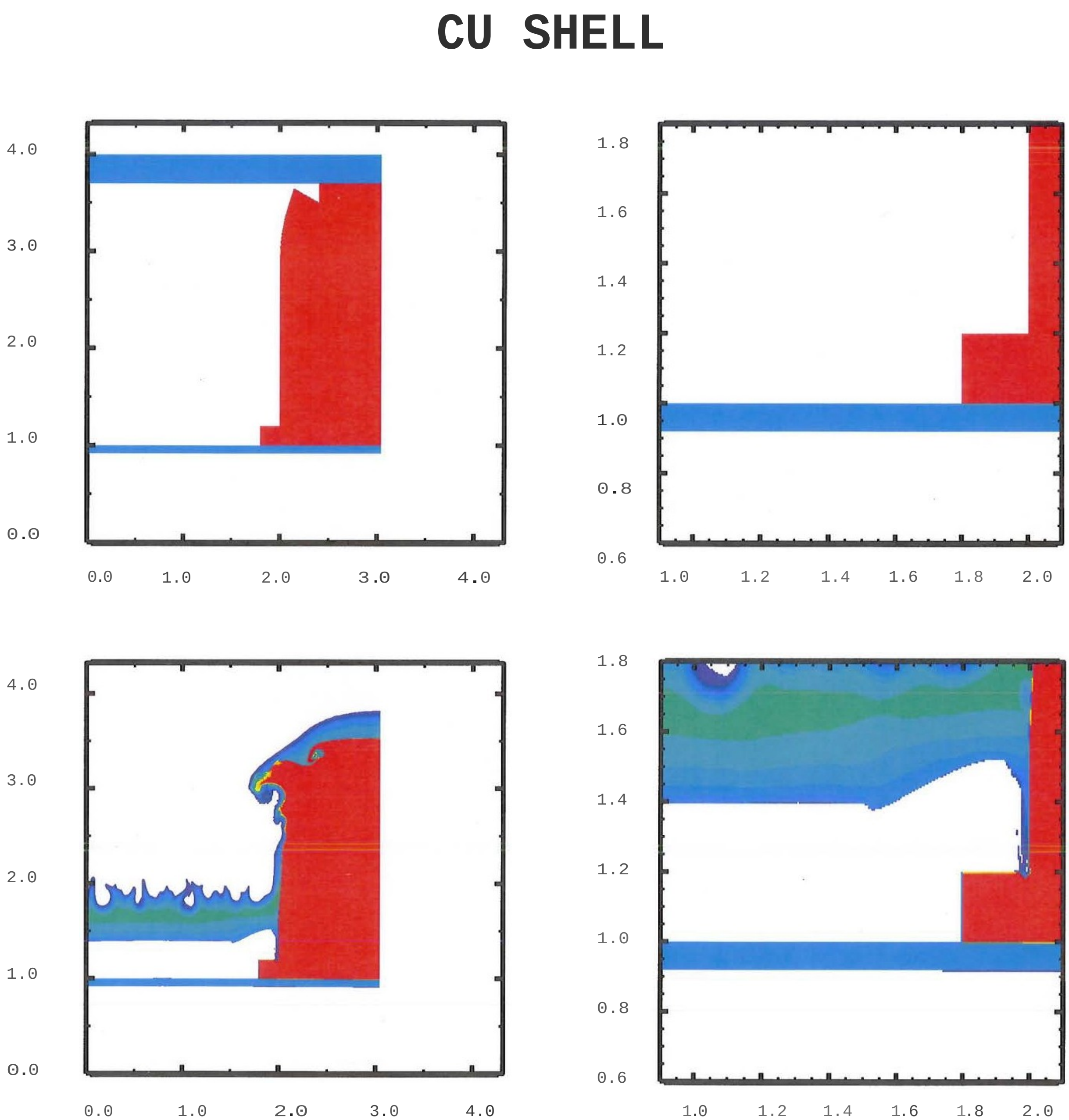

Figure 12. Target-Liner Interaction with CU ring surrounding Target. Top row: initial conditions. A CU ring surrounds target near the glide plane. Bottom row: tip of jet reaches the ring. Jet is far in front of rest of liner.

Figure 13 shows the interaction continuing. As in the previous simulation, the top row shows the jet slowing down as it plows through ring while the rest of liner starts to catch up. The bottom row shows the jet still restrained by ring while the rest of liner starts to pass the jet.

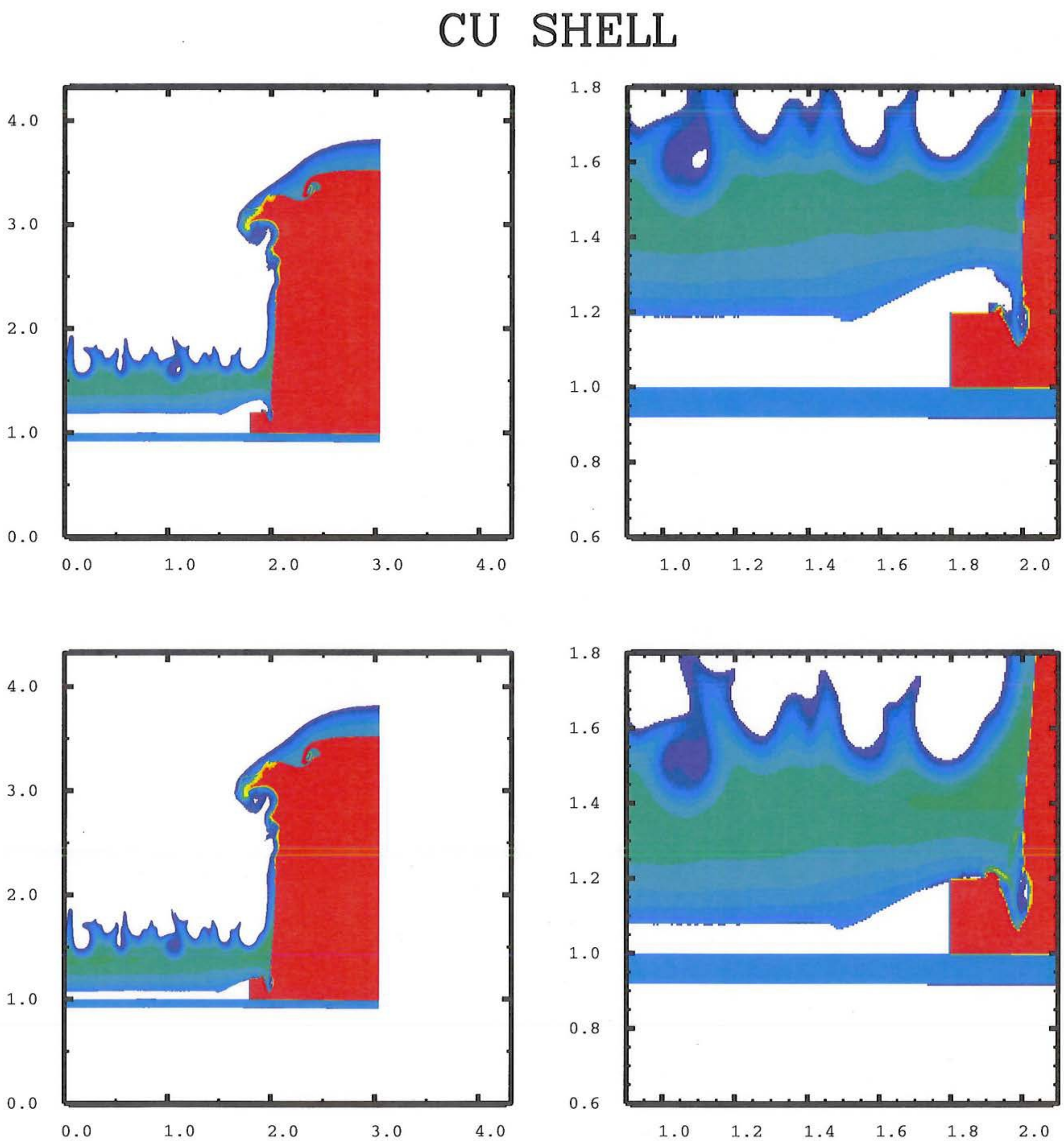

Figure 13. The interaction Continues. Top: Jet slows down as it plows through ring. Rest of liner starts to catch up. Bottom: Jet still restrained by ring. Rest of liner starts to pass the jet.

Interaction Concludes – Jet does not interfere with Measurement

Figure 14 shows the conclusion of the simulation. After the liner hits the target and the shock is half way through (top row), the jet is still constrained by the shell. The bottom row shows the liner almost reaching the top of CMU position while the jet is still constrained by the ring. Thus, the CU ring also prevents the jet from interfering with the measurement.

Several other simulations have shown that any sufficient amount of mass intercepting the jet will constrain it for enough time for the measurements to be viable.

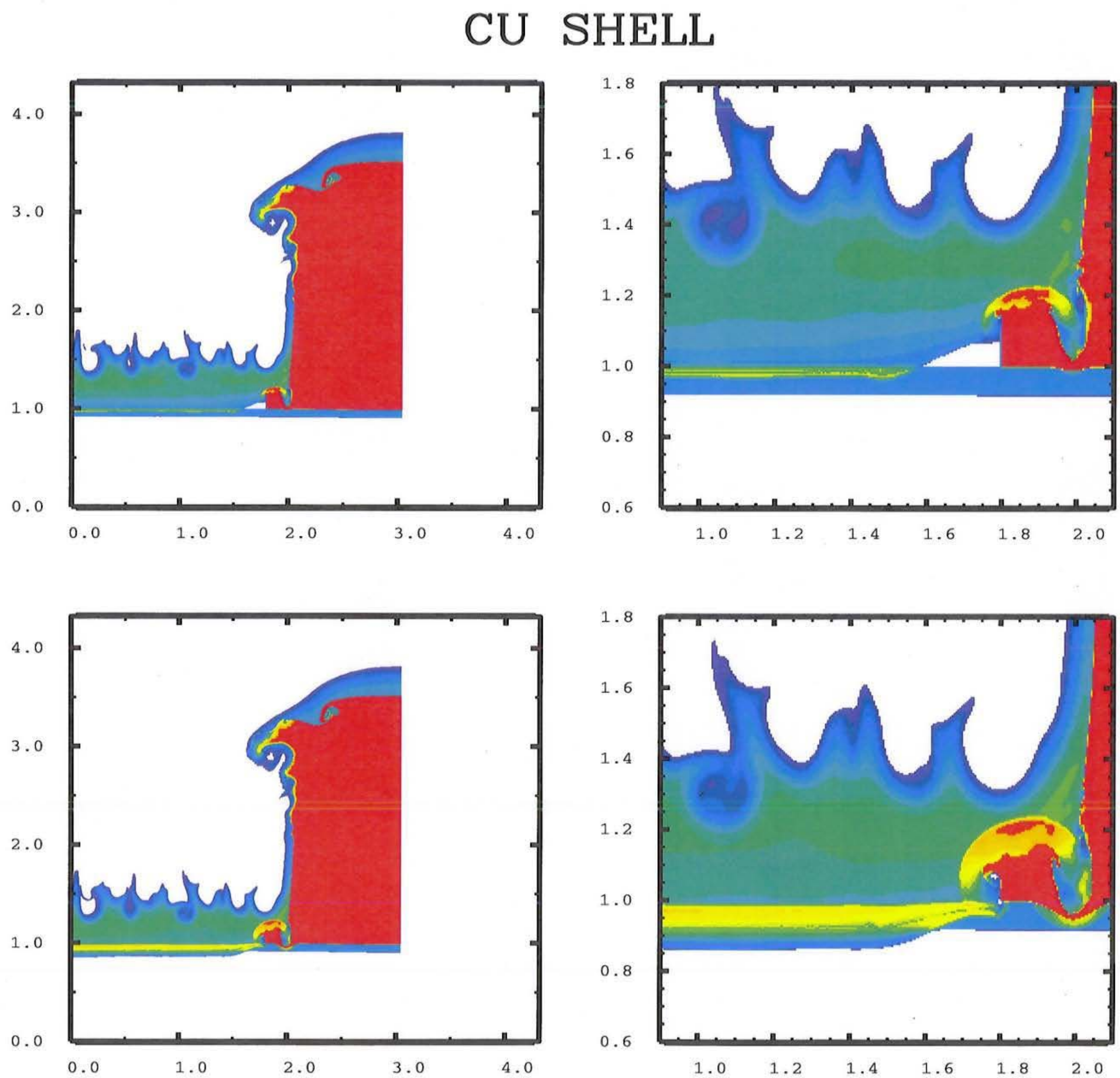

Figure 14. Interaction Concludes – Jet does not interfere with Measurement. Top: Liner hits target and shock is half way through. Bottom: Liner almost reaches top of CMU position. Experiment almost over. Jet still constrained by ring and does not interfere with measurement.

Target-Liner Interaction – Conclusions

- The interaction of the liner with the GP (as designed) results in a jet of fast liner material next to the GP which outruns the rest of the liner.
- If the jet motion is not mitigated, the jet smashes through the target before the main part of the liner reaches the target. The jet and associated target material reach the CMU position before the shock from the main part of the liner interaction brakes out. So the measurements are potentially compromised even before they begin.
- Any piece of high density metal outside the target near the GP will slow down the jet.

The Main part of the liner then passes the jet and hits the target. The resulting shock breaks out of the inner target surface and the desired signal can be measured by the CMU without being compromised.

- The tooth notch (A. Buyko[10]) should work well for this purpose.
- A high density ring just outside the target next to the GP also should work well.
- The deciding considerations may be ease of manufacture and the predicted qualities of the inner target surface (such as smoothness and uniformity) as it approaches the CMU.
- Our previously reported results[11] (at the XV Khariton conference) of 1D target-liner interactions found that in the «computational» aluminum forming the target:
  - ○ The post transmitted shock density is about 6.2 gm/cc;
  - ○ The post transmitted shock material velocity $v_p = 1.15 \pm 0.05$ cm/μs;
  - ○ The transmitted shock velocity $v_s = 1.7 \pm 0.1$ cm/μs;
  - ○ $v_s / v_p = 1.5$;
  - ○ Just before impact, the inner 0.1 cm of the liner and the part of the liner beyond
  - ○ 1.5 cm are melted;
  - ○ The target expands and melts as it implodes. The inner target surface velocity increases quickly to 2.4 cm/μs, which is velocity of the inner liner surface just before contact, 2.1 cm/μs, increased by $1/r$.
  - ○ The initial evaluation of the 2D simulations are consistent with these results.
  - ○ The experiment will measure these quantities in "real" aluminum.

References

1. Buyko A. M., Gorbachev Yu. N., Zmushko V. V. et alia "Simulation of Atlas parameters in explosive magnetic experiments ALT-1,2", Proc. of 9th Int. Conf. on Meg. Mag. Field Gen. and Related Topics. M.–St.Pet. 2002, Eds. V. D. Selemir and L. N. Plyashkevich, Sarov, VNIIEF, 2004. P. 747–751.
2. Sgro A. G., and Atchison W. L. "Simulation of Magnetically Driven Experiments" Proc. XIII Khariton Scientific Talks. Ed. A. L. Mikhailov, RFNC-VNIIEF, Sarov, 2011. P. 211–221.
3. Buyko A. M., Garanin S. F., Glybin A. I. et alia "A Disk EMG System for Driving Impacting Liners to ~20 km/s", Proc. XIII Khariton Scientific Talks. Ed. A. L. Mikhailov, RFNC-VNIIEF, Sarov, 2011. P. 488–495.
4. Buyko A. M., Garanin S. F., Zmushko V. V. et alia "Simulations of Magnetic Implosion of Impacting Liners Driven to ~20 km/s". Proc. XIII Khariton Scientific Talks. Ed. A. L. Mikhailov, RFNC-VNIIEF, Sarov, 2011. P. 549–556.
5. Buyko A. M., Garanin S. F., and Zmushko V. V. "Magnetic liner implosion simulations for the ALT-3 experiment", Pres. XIV Int.Conf. Khariton Scientific Talks. RFNC-VNIIEF, Sarov, 12–16 March 2012.
6. Buyko A. M., Garanin S. F., and Zmushko V. V. "Magnetic liner implosion simulations for the ALT-3 experiment", Report at the XIV Intern. Conf. on Megagauss Magn. Field Generation and Related Topics. October 14–19, 2012, USA, Hawaii, Maui.
7. Miles A. R. "Simulation of liner uniformity in the ALT-3 test problem", Report at the XIV Intern. Conf. on Megagauss Magn. Field Generation and Related Topics. October 14–19, 2012, USA, Hawaii, Maui.
8. Miles A. R. "Simulation of liner uniformity in the ALT-3 liner test problem", Presented at the XV Khariton Scientific Readings.
9. Buyko A. M., Garanin S. F., and Zmushko V. V. "To the Choice of Liner PU Geometry for the ALT-3 Experiment", Presented at the XV Khariton Scientific Readings.
10. Buyko A. M., Private communication.
11. Sgro A. G., Rousculp C. L., and Reinovsky R. E. "ALT-3 Implosion Analysis", Presented at the XV Khariton Scientific Readings.